ARTICLE

Applied Polymer SCIENCE WILEY

Effect of vortex-induced physical stress on fluorescent properties of dye-containing poly(ethylene glycol)-*block*-poly(lactic acid) micelles

Tyler L. Odom[1] | Jacob R. Blankenship[1] | Giselle Campos[1] | Devin C. Mart[1] |
Wenyan Liu[2,3] | Risheng Wang[3] | Keiichi Yoshimatsu[1]

[1]Department of Chemistry, Missouri State University, Springfield, Missouri

[2]Center for Research in Energy and Environment, Missouri University of Science and Technology, Rolla, Missouri

[3]Department of Chemistry, Missouri University of Science and Technology, Rolla, Missouri

Correspondence
Keiichi Yoshimatsu, Department of Chemistry, Missouri State University, Springfield, MO 65897
Email: kyoshimatsu@missouristate.edu

Abstract

The effect of vortex-induced mechanical stresses on the fluorescent properties of dye-containing poly(ethylene glycol)-*block*-poly(lactic acid) (PEG-*b*-PLA) block copolymer micelles has been investigated. PEG-*b*-PLA block copolymer micelles containing fluorescent dyes, 3,3′-dioctadecyloxacarbocyanine perchlorate (DiO) and/or 1,1′-dioctadecyl-3,3,3′,3′-tetramethylindocarbocyanine perchlorate (DiI), are prepared by a simple one-step procedure that involves the self-assembly of block copolymers and spontaneous incorporation of hydrophobic dyes into the core of the micelles. Upon vortexing, the micelle dispersion samples showed a decrease in fluorescence intensity in a rotational speed- and time-dependent manner. The results demonstrated that the vortexing can alter the fluorescent properties of the dye-containing PEG-*b*-PLA block copolymer micelle dispersion samples, suggesting the potential utility of block copolymer micelles as a mechanical stress-responsive nanomaterial.

KEYWORDS

micelles, self-assembly, stimuli-sensitive polymers

1 | INTRODUCTION

Mechanical stresses ubiquitously occur on objects in motion. Along these lines, synthetic nanomaterials with stimuli-responsive properties to such mechanical stresses have attracted a great interest[1–6] for the potential utilities in broad areas as mechano-responsive chromic/luminescent materials,[2–5] self-healing and self-immolative materials,[4,7] drug delivery nanocarriers,[6,8–10] protein-releasing nanocontainers for bioreactors,[11] and nanoprobes for biomechanical research.[12–14] In the development of mechanical stress-responsive nanomaterials, it

is important to establish understanding of the properties of nanomaterials upon exposure to mechanical stresses. We here report the effect of vortex-induced mechanical stresses on the fluorescent properties of dye-containing poly(ethylene glycol)-*block*-poly(lactic acid) (PEG-*b*-PLA) block copolymer micelles.

To date, a number of studies have described the influence of mechanical stresses, such as shear and elongational forces on the morphologies of block copolymer micelles. For example, it has previously shown that agitation can trigger deformation/transformation of micellar structures[15–21] (e.g., from cylinders to rings,[18]

from spheres to rods[21]). In addition, there have been reports on the loss of gene delivery efficiency by block copolymer micelle-based nanocarriers due to the shear stress-induced structural deterioration,[21] the preparation of bulk hydrogel by crosslinking of block copolymer micelles for mechanical stretching-induced drug release,[22] and the vortex-induced acceleration of the polymer chain exchange between block copolymer micelles.[23] However, little has been reported in regard with the effect of mechanical stresses on the fluorescent properties of dye-containing copolymeric micelles.[24]

In this work, we focused on the behavior of fluorescent dye-containing PEG-*b*-PLA block copolymer micelles upon exposure to vortex-induced mechanical stresses. The dye-containing micelles were prepared in a simple one-step procedure by capitalizing the unique capability of amphiphilic block copolymers to spontaneously self-assemble into micellar forms and incorporate hydrophobic "guest" molecules into their interior.[25–30] Our results demonstrate that the vortexing causes the decrease of fluorescence intensity of the prepared micelle dispersion samples in a rotational speed- and time-dependent manner, showing the promising properties of copolymer micelles as a new mechanical stress-responsive nanomaterial.

2 | EXPERIMENTAL

2.1 | Materials

Poly(ethylene glycol)-*block*-poly(lactic acid) (PEG(5000)-*b*-PLA(5000), PEG-*b*-PLA) was purchased from Polysciences Inc. (Warrington, PA). 3,3′-Dioctadecyloxacarbocyanine perchlorate (DiO) was purchased from Marker Gene Technologies, Inc. (Eugene, OR). 1,1′-Di-*n*-octadecyl-3,3,3′,3′-tetramethylindocarbocyanine perchlorate (DiI) was purchased from Alfa Aesar (Lancashire, UK). Deuterium oxide (D_2O, 99.8 atom % D) and deuterated acetone (acetone-d_6, 99.8 atom % D) were purchased from Acros Organics (Geel, Belgium). The standard grade regenerated cellulose dialysis tubing (Spectra/Por 6, molecular weight cutoff [MWCO]: 3.5 kDa, 18 mm flat width) was purchased from Repligen Corporation (Waltham, MA). Carbon film-coated Cu TEM grids (300 mesh, 01843-F) were purchased from Ted Pella, Inc. (Redding, CA).

2.2 | Preparation of dye-containing block copolymer micelles

Micelles were prepared by following the previously reported procedures[31–33] with minor modifications. One milliliter of the acetone solution containing PEG-*b*-PLA block copolymer (10.0 mg), DiO (0.015 mg), and DiI (0.075 mg) was prepared by mixing stock solution of each component (See Supporting Information for more detail on the procedure). The solution was added dropwise into 5 ml of deionized water in a 20-ml borosilicate glass scintillation vial under vigorous stirring (300 rpm). The solution was then kept under stirring for 3 h at room temperature to vaporize acetone. The obtained supernatant was then transferred into a dialysis unit equipped with a dialysis membrane (Spectra/Por 6, molecular weight cutoff [MWCO]: 3.5 kDa, 18 mm flat width) and was dialyzed against 500 ml of deionized water for 2 days. Deionized water was changed after 1 day. The dialyzed samples were stored in a 15-ml polypropylene tube at 4°C until the time of use.

2.3 | Determination of block copolymer concentration

After dialysis, the concentration of the block copolymer in the obtained micelle sample was determined by gravimetric analysis. Two to three milliliters of the sample was lyophilized and the weight of dry polymers was measured on an analytical balance. The measured dry weight of the obtained polymer was divided by the initial volume of the solution to calculate the polymer concentration of the sample.

2.4 | Fluorescence measurement

The fluorescence spectra were measured on a QuantaMaster spectrofluorometer (Photon Technology International, Inc. Birmingham, NJ) with integration time of 1 s, and increment of 1 nm. A 3-ml quartz cuvette (internal dimension: 10 mm × 10 mm) was used in all measurements.

2.5 | UV–visible absorption measurement

The UV–visible absorption spectra of samples were measured on a Cary 60 spectrophotometer (Agilent Technologies, Santa Clara, CA) or a cuvette port of SpectraMax M5 multi-mode microplate reader (Molecular Devices, Sunnyvale, CA). A 1-ml quartz cuvette with a 10 mm path length was used in all measurements. Prior to the absorption measurement, micelle samples were diluted to 1.00 mg ml^{-1} in water or 0.667 mg ml^{-1} in acetone: water (2:1, vol/vol).

2.6 | Transmission electron microscope measurement

Transmission electron microscopy (TEM) images were acquired on a Tecnai F20 field-emission electron microscope (FEI Company, Hillsboro, OR) at an acceleration voltage of 200 kV. Prior to the preparation of the sample, a carbon film-coated Cu TEM grid was glow-discharged by a plasma cleaner. Three microliters (3 μl) of the micelle samples (0.25 mg polymer/ml) was dropped onto the glow-discharged grid. Water remained on the surface of the TEM grid after 3 min of incubation was absorbed with a piece of Kimwipes® and air-dried at room temperature. The size of block copolymer micelles on TEM images were quantified by using ImageJ software (NIH).[34–36]

2.7 | Typical procedure for determining the effect of vortexing

A typical procedure for determining the effect of vortexing is as follows: A 25 ml of 5.00 μg ml^{-1} dye-containing block copolymer micelle sample was prepared by mixing appropriate amounts of the stock micelle solution and water. To a series of 15-ml polypropylene centrifuge tubes, 3 ml of the micelle samples (5.00 μg ml^{-1}) were transferred using a micropipettor. Three tubes are attached to a Digital Vortex-Genie 2 (Scientific Industries, Inc., Bohemia, NY) equipped with a vertical high-speed 15-ml tube holder. Out of six holding arms, every other arm was left empty to ensure the stable rotation of the tube holder. Each tube was located at 2.7 cm from the center of the vortexer and rotated in a circular orbit with a radius of 2.3 mm. After vortexing, all solution in the tube was transferred to a 3-ml quartz cuvette and the fluorescence spectrum was measured with the setting described above.

3 | RESULTS AND DISCUSSION

3.1 | Critical micelle concentration and ^{1}H NMR characterization

Critical micelle concentration (CMC) is the concentration above which an ionic or nonionic surfactant forms micellar structures. The CMC of the PEG-*b*-PLA block copolymer was determined by measuring the fluorescence of pyrene in the presence of varied concentrations of the block copolymer.[37,38] The determined CMC value was 19 μg ml^{-1} (Figure S1), which was close to the CMC value reported for a PEG-*b*-PLA block copolymer

consisting of similar block lengths on literature.[37] ^{1}H NMR measurements were performed to determine the chain mobility of each block within micellar structure since both temperature and chain lengths of PEG and PLA blocks affect the behavior of PEG-*b*-PLA block copolymer micelles.[37,39] The results showed that CH$_2$ peaks (3.7–4.3 ppm) in PEG block can be observed in the spectra acquired at 25–70°C whereas CH$_3$ peaks (1.3–2.3 ppm) from PLA block could only be observed at 40°C and higher (Figures S2-S4 and Table S1). This indicates that the PEG block is highly solubilized in water at all these temperatures. On the other hand, the PLA block is forming a "solid-like" core with low chain mobility at room temperature.[39]

3.2 | Preparation of dye-containing block copolymer micelles

Hydrophobic dye-containing amphiphilic block copolymer micelles have been previously used in several studies on the dye transfer from micelles to biological membranes,[31] proteins,[33,40] and/or dye exchange between micelles.[32] In this study, we adapted DiO and/or DiI-containing PEG-*b*-PLA block copolymer micelles as a model system in order to investigate the effect of vortexing-induced mechanical stresses on the fluorescent properties of dye-containing block copolymer micelles (Figure 1).

For this purpose, the three block copolymer micelles were prepared: two contained either DiO or DiI dye; and one contained both DiO and DiI dyes. The DiO/PEG-*b*-PLA and DiI/PEG-*b*-PLA micelle samples showed a fluorescence emission peak at 507 nm (DiO emission peak) and 568 nm (DiI emission peak), respectively (Figure 2(a,
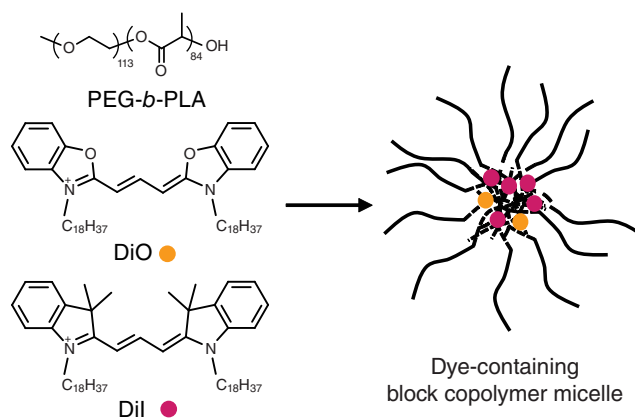
FIGURE 1 Schematic illustration of dye-containing block copolymer micelles. The illustration of a DiO/DiI/PEG-*b*-PLA block copolymer micelle is described above as an example [Color figure can be viewed at wileyonlinelibrary.com]
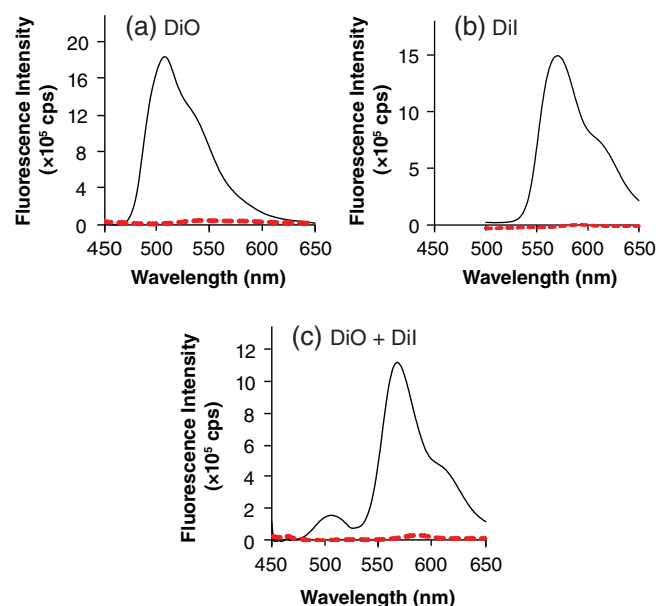
FIGURE 2 Fluorescence emission spectra of solution prepared by dropwise addition of (a) DiO, (b) DiI, and (c) DiO and DiI into water with or without PEG-*b*-PLA block copolymer. The spectrum was measured with an excitation light of 425 nm for (a) DiO and (c) DiO + DiI with an excitation light of 475 nm for (b) DiI. Solid line (black): With PEG-*b*-PLA block copolymer. Dashed line (red): Without block copolymer [Color figure can be viewed at wileyonlinelibrary.com]

b), solid lines). On the DiO/DiI/PEG-*b*-PLA micelles containing two dyes, a small peak at 507 nm was observed but the dominant peak was found at 568 nm, indicating the occurrence of Förster resonance energy transfer (FRET) from DiO to DiI[24,31,32,38,40–43] (Figure 2(c), solid line). As FRET occurs only when DiO (donor dye) and DiI (acceptor dye) are present within a few nanometers of each other,[43] the result confirmed the formation of block copolymer micelles and incorporation of these hydrophobic dyes into the micellar core.[31] The amount of the DiO and DiI dyes in each micelle dispersion sample

was determined based on the UV–visible absorption spectra (Table 1).

3.3 | Fluorescent spectral change induced by vortexing

Our hypothesis was that the mechanical stresses induced by vortexing would trigger the release of the dyes that are kinetically entrapped in the solid-like core of the micelles. The release of the dyes into a more polar solution phase should yield detectable changes (e.g., solvatochromic shift of emission peaks or change in FRET efficiency[43]) in the fluorescence spectrum. To test the hypothesis 3 ml of the DiO/PEG-*b*-PLA, DiI/PEG-*b*-PLA, and DiO/DiI/PEG-*b*-PLA micelle samples were diluted to 5 µg ml^{-1} in H$_2$O, which is below the CMC, in a 15-ml conical polypropylene centrifuge tube and were subjected to vortexing at 3000 rpm for 5 min. Somewhat interestingly, instead of the shift of emission peaks or change in FRET efficiency, we observed the decrease in the height of both donor (DiO) and acceptor (DiI) peaks upon vortexing for all the dye-containing micelle dispersion samples (Table 1 and Figure S6). A similar trend was observed with samples containing higher concentrations of DiO/DiI/PEG-*b*-PLA micelles. Meanwhile, the degree of the vortex-induced fluorescence intensity decrease was less pronounced for these samples. The fluorescence intensity decreased by 33.2% at 50 µg ml^{-1} after vortexing at 3000 rpm for 5 min and by 21.9% at 250 µg ml^{-1} after vortexing at 3000 rpm for 10 min (data not shown).

3.4 | Behavior and morphology of dyes and micelles in aqueous solution

To better understand the observed spectral change a series of experiments were carried out. To this end, we investigated the behavior of DiO and DiI dyes in aqueous

TABLE 1 Dye content and percentage of fluorescence intensity decrease after vortexing at 3000 rpm for 5 min of dye-containing PEG-*b*-PLA block copolymer micelle dispersions

	DiO, feed (wt%)[a]	DiI, feed (wt%)[a]	DiO, Found[b] (wt%)[a]	DiI, found[b] (wt%)[a]	Fluorescence decrease upon vortexing (% ± SD[c])
DiO/PEG-*b*-PLA	0.15	—	0.12	—	56 ± 10
DiI/PEG-*b*-PLA	—	0.75	—	0.43	49 ± 5
DiO/DiI/PEG-*b*-PLA	0.15	0.75	0.11	0.49	40 ± 4

[a]Based on the ratio of the weight of dye to the weight of polymer.
[b]Determined from UV–visible absorbance spectra.
[c]Calculated standard deviation (*n* = 3).

solution in the absence of block copolymers, stability of micelles over an extended time period and under different temperatures, and morphology of the block copolymer micelles.

### 3.4.1 | Behaviors of DiO and DiI dyes in absence of polymer

It has been previously reported that both DiO and DiI dyes are soluble in acetone but these dyes show little to no solubility in water.[32,44,45] Therefore, fluorescence properties of DiO and DiI dyes in the absence of block copolymer micelles were studied. Our control experiment confirmed that both DiO and DiI dyes were soluble in acetone and the obtained solution showed fluorescence emission peak at 507 and 568 nm, respectively. We then repeated the procedure for the micelle sample preparation but without the block copolymer. It was observed that most of DiI dyes adhered to the surface of magnetic stirring bars and glass vials during the dropwise addition of acetone solutions containing DiI into deionized water and subsequently acetone vaporization. On the other hand, it was found that DiO forms colloidally stable aggregates in water as the sample retained the yellow color even after dialysis. Meanwhile, the supernatants of neither DiO nor DiI samples exhibited any fluorescence when those dyes were added into water without block copolymers (Figures 2(a–c), dashed lines), indicating that these dyes are not fluorescent in aqueous environments unless the dyes are incorporated in block copolymer micelles. These results suggested that a decrease in the fluorescence intensity could be caused by the precipitation and/or aggregation of the dyes that are released to aqueous phase. This explanation appears to be consistent with the less pronounced effects of vortexing at the high micelle concentrations as the higher micelle concentrations could increase the probability for the dyes being reabsorbed by other micelles.

3.4.2 | Fluorescence measurement over extended time period and under different temperatures

To gain more insights on the stability of the block copolymer micelles in static conditions, the fluorescence measurement experiment with the dye-containing micelle dispersions was repeated with an extended incubation period at room temperature. In the first part of this experiment, the diluted micelle samples (5 μg polymer ml^{-1}) were incubated for 5 h under static conditions and the fluorescence spectra were acquired at 1 hour-intervals. Despite that the micelle samples were diluted to below the CMC of the block copolymer, the fluorescence intensity of the samples showed little change over 5 h until being subjected to vortexing (Figure 3). This confirmed the kinetic stability of the dye-containing micelles in the diluted conditions. In other words, the PEG-*b*-PLA block copolymer micelles are, once formed, highly stable under static conditions unless they are exposed to vortexing, presumably due to the "solid-like" nature of the micelle core. Indeed, we found that the stock solution of dye-containing micelles (2 mg ml^{-1}) stored at 4°C did not show any noticeable spectral change over several weeks. The fluorescence intensity largely decreased upon 5 min of vortexing at 3000 rpm and it remained at the same level during 2 h of the subsequent static incubation time. This apparently implies that the observed decrease in the fluorescence intensity is irreversible.

In addition, we investigated the stability of micelles at higher temperatures. In contrast to the micelle samples incubated at room temperature, the samples incubated at 38 and 60°C showed an irreversible decrease of fluorescence intensity even without vortexing (Table S4). This appears to indicate that the low chain mobility of the PLA block contributes to the stability of the dye-containing micelles at room temperature. It was also observed that vortexing of dye-containing micelle samples at 38°C resulted in further decrease of fluorescence intensity. Despite that vortexing of micelle samples at higher temperatures could not be performed due to the limitations of the current setup of our equipment, the results suggested that the behavior of block copolymer micelles could be affected by temperature.
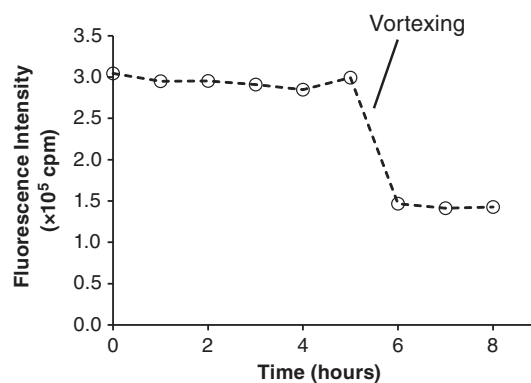
FIGURE 3 Change in fluorescence intensity of DiO/DiI/PEG-*b*-PLA micelle samples over time. The samples were incubated statically for 5 h followed by 5 min of vortexing at 3000 rpm and subsequent static incubation.) excitation wavelength: 425 nm. Emission wavelength: 567 nm

3.4.3 | TEM analysis

In order to analyze the effect of vortexing from the viewpoint of the micelle morphology, the block copolymer micelle samples were characterized by TEM. Figure 4 shows the size distribution of the DiO/DiI/PEG-*b*-PLA micelle samples before and after being subjected to vortexing at 3000 rpm for 5 min. The average diameter of DiO/DiI/PEG-*b*-PLA micelles before vortexing was 17.5 nm with the standard deviation of 4.0 nm ($n = 91$) and the size distribution of the micelles was mono-modal. In contrast, the size distribution pattern was significantly different for the micelles being subjected to vortexing; micelles with larger sizes could be observed and the average diameter also increased to 22.7 nm with the standard deviation of 10.7 nm ($n = 180$).

The change in the size distribution of micelles suggests that the vortex-induced mechanical stresses cause the fusions of the micelles. Meanwhile, it is important to note that it was technically challenging to detect micelles below 9 nm due to the low contrast compared to the background. Therefore, we could not accurately quantify the number of smaller micelles. For this reason, the occurrence of the fission of the micelles, release of dyes, or expulsion of polymer chains into solution phase could not be either confirmed or excluded.

Overall, the result of TEM measurements showed that the vortex-induced mechanical stresses are sufficiently strong to trigger the morphological changes of the block copolymer micelles. Based on this observation along with other data, we attributed the vortex-induced fluorescence decrease to the aggregation and/or precipitation of the DiO and DiI dyes that are released into the aqueous phase.
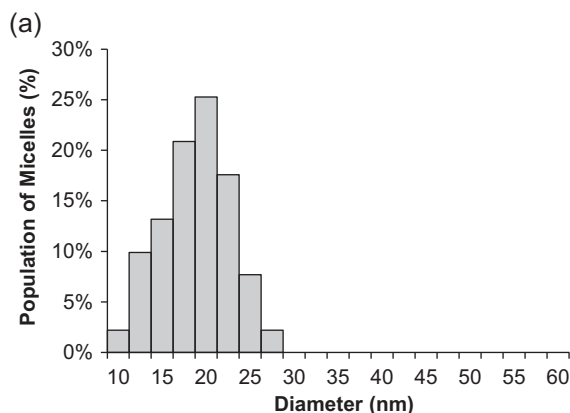
3.5 | Correlation between rotational speed and rate of spectral change

Finally, the correlation between the rotational speed and the rate of spectral change was investigated. In these experiments, we focused on the DiO/DiI/PEG-*b*-PLA block copolymer micelles. This was because the use of the donor/acceptor pair provides more information in terms of the colocation of DiI and DiO dyes, even though the micelles containing only one of these dyes also showed the decrease in the fluorescence intensity upon vortexing.

Figure 5 presents the fluorescence intensity of the DiO/DiI/PEG-*b*-PLA micelle samples that are subjected to vortexing at different speeds for 5 min. As it is shown,
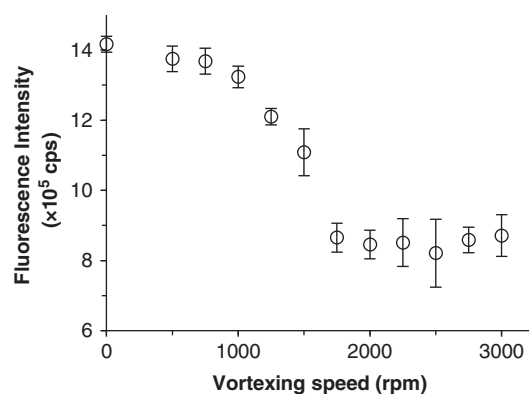
FIGURE 5 Fluorescence emission intensity of DiO/DiI/PEG-*b*-PLA block copolymer micelle samples that are subjected to vortexing at 0, 500, 750, 1000, 1250, 1500, 1750, 2000, 2250, 2500, 2750, and 3000 rpm for 5 min. Excitation wavelength: 425 nm. Emission wavelength: 567 nm
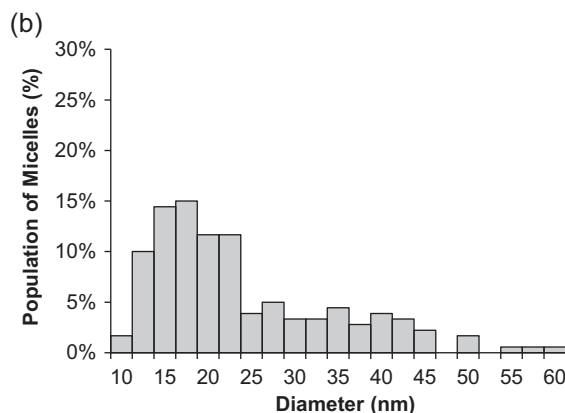
FIGURE 4 Size distribution of the DiO/DiI/PEG-*b*-PLA block copolymer micelles a) before ($n = 91$) and b) after ($n = 180$) being subjected to vortexing at 3000 rpm for 5 min on transmission electron micrographs

the fluorescence intensity noticeably decreases upon the 5 min of vortexing at 1000 rpm and higher speed, whereas vortexing at 750 rpm or lower speeds does not significantly affect the fluorescent properties of the micelles. Between 1000 and 1750 rpm, the amount of fluorescence intensity change varied in a rotational speed-dependent manner. These observations suggest that the decrease of the fluorescence intensity occurs only when the mechanical stresses are above a certain threshold value. The effect reached a plateau when rotational speeds exceeded 1750 rpm.

The rate of vortex-induced fluorescence intensity change was studied by measuring the fluorescence spectra of the micelle samples that were subjected to vortexing over different durations. As shown in Figure 6, the fluorescence intensity decreased as the duration of vortexing increased. The data points were fitted by using Equation (1):

$$I = Ae^{-\frac{t}{\tau}} + B \tag{1}$$

where I is the fluorescence intensity at each time point, t is time; τ is a rate constant, and A and B are fitting parameters. The rate constants (τ) that were extracted from the fitting are 4.23 and 1.46 min^{-1} for the rotational speeds at 1500 and 3000 rpm, respectively, showing that the fluorescence intensity decreases at a faster rate as the rotational speed increases. It was also noteworthy that a clearly noticeable decrease in the fluorescence intensity could be observed after as little as 30 s of vortexing at 3000 rpm.
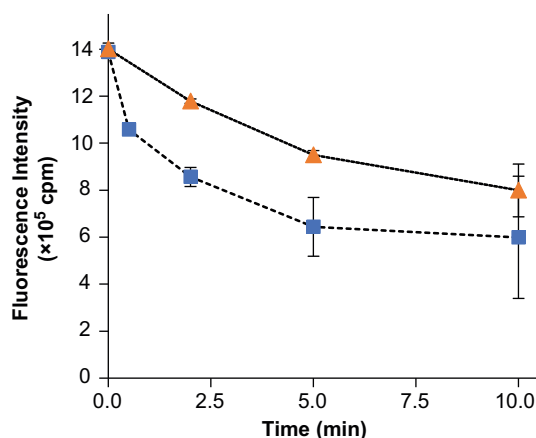
FIGURE 6 Time course of fluorescence emission intensity of DiO/DiI/PEG-*b*-PLA block copolymer micelle samples that are subjected to vortexing at 3000 rpm (square, blue) and 1500 rpm (triangle, orange) over 10 min. Excitation wavelength: 425 nm. Emission wavelength: 567 nm [Color figure can be viewed at wileyonlinelibrary.com]

4 | CONCLUSIONS

In this work, we investigated the effect of vortex-induced mechanical stresses on the fluorescent properties of dye-containing block copolymer micelles. The dye-containing micelle dispersion samples showed a decrease of the fluorescence intensity upon vortexing at 1000 rpm or higher speeds, while the micelles are highly stable in static conditions. The TEM analysis showed that the vortex-induced mechanical stresses could induce morphological changes of the micelles. The results also showed that the vortex-induced mechanical stresses can alter the fluorescent properties of the dye-containing PEG-*b*-PLA block copolymer micelle dispersions in a rotational speed and time-dependent manner. Building upon the current findings, we are envisioning to develop a library of block copolymer micelles with different mechanical stress-responsive profiles that would meet various requirements in application settings.

ORCID
Wenyan Liu https://orcid.org/0000-0002-7233-7601
Risheng Wang https://orcid.org/0000-0001-6539-1565
Keiichi Yoshimatsu https://orcid.org/0000-0002-1428-0029

REFERENCES
[1] K. Ariga, T. Mori, J. P. Hill, *Adv. Mater.* **2012**, *24*, 158.
[2] Z. Chi, X. Zhang, B. Xu, X. Zhou, C. Ma, Y. Zhang, S. Liu, J. Xu, *Chem. Soc. Rev.* **2012**, *41*, 3878.
[3] A. J. McConnell, C. S. Wood, P. P. Neelakandan, J. R. Nitschke, *Chem. Rev.* **2015**, *115*, 7729.
[4] J. Li, C. Nagamani, J. S. Moore, *Acc. Chem. Res.* **2015**, *48*, 2181.
[5] Y. Sagara, S. Yamane, M. Mitani, C. Weder, T. Kato, *Adv. Mater.* **2016**, *28*, 1073.
[6] P. Cai, B. Hu, W. R. Leow, X. Wang, X. J. Loh, Y.-L. Wu, X. Chen, *Adv. Mater.* **2018**, *30*, 1800572.
[7] M. B. Larsen, A. J. Boydston, *Macromol. Chem. Phys.* **2016**, *217*, 354.

[8] M. N. Holme, I. A. Fedotenko, D. Abegg, J. Althaus, L. Babel, F. Favarger, R. Reiter, R. Tanasescu, P.-L. Zaffalon, A. Ziegler, B. Müller, T. Saxer, A. Zumbuehl, *Nat. Nanotechnol.* **2012**, *7*, 536.

[9] N. Korin, M. Kanapathipillai, B. D. Matthews, M. Crescente, A. Brill, T. Mammoto, K. Ghosh, S. Jurek, S. A. Bencherif, D. Bhatta, A. U. Coskun, C. L. Feldman, D. D. Wagner, D. E. Ingber, *Science* **2012**, *337*, 738.

[10] T. Saxer, A. Zumbuehl, B. Müller, *Cardiovasc. Res.* **2013**, *99*, 328.

[11] T. Natsume, M. Yoshimoto, *ACS Appl. Mater. Interfaces* **2014**, *6*, 3671.

[12] W. J. Polacheck, C. S. Chen, *Nat. Methods* **2016**, *13*, 415.

[13] Y. Liu, K. Galior, V. P.-Y. Ma, K. Salaita, *Acc. Chem. Res.* **2017**, *50*, 2915.

[14] P. Roca-Cusachs, V. Conte, X. Trepat, *Nat. Cell Biol.* **2017**, *19*, 742.

[15] K. I. Winey, S. S. Patel, R. G. Larson, H. Watanabe, *Macromolecules* **1993**, *26*, 2542.

[16] K. Mortensen, E. Theunissen, R. Kleppinger, K. Almdal, H. Reynaers, *Macromolecules* **2002**, *35*, 7773.

[17] B. Lonetti, J. Kohlbrecher, L. Willner, J. K. G. Dhont, M. P. Lettinga, *J. Phys. Condens. Matter* **2008**, *20*, 404207.

[18] H. Yu, W. Jiang, *Macromolecules* **2009**, *42*, 3399.

[19] M. Zhang, M. Wang, S. He, J. Qian, A. Saffari, A. Lee, S. Kumar, Y. Hassan, A. Guenther, G. Scholes, M. A. Winnik, *Macromolecules* **2010**, *43*, 5066.

[20] C.-W. Wang, D. Sinton, M. G. Moffitt, *ACS Nano* **2013**, *7*, 1424.

[21] K. M. Takeda, Y. Yamasaki, A. Dirisala, S. Ikeda, T. A. Tockary, K. Toh, K. Osada, K. Kataoka, *Biomaterials* **2017**, *126*, 31.

[22] L. Xiao, J. Zhu, J. D. Londono, D. J. Pochan, X. Jia, *Soft Matter* **2012**, *8*, 10233.

[23] R. P. Murphy, E. G. Kelley, S. A. Rogers, M. O. Sullivan, T. H. Epps, *ACS Macro Lett.* **2014**, *3*, 1106.

[24] J. Zhu, M. Tan, L. Zhang, Q. Yin, *Soft Matter* **2014**, *10*, 6506.

[25] Y. Mai, A. Eisenberg, *Chem. Soc. Rev.* **2012**, *41*, 5969.

[26] R. Z. Xiao, Z. W. Zeng, G. L. Zhou, J. J. Wang, F. Z. Li, A. M. Wang, *Int. J. Nanomed.* **2010**, *5*, 1057.

[27] E. V. Batrakova, A. V. Kabanov, *J. Controlled Release* **2008**, *130*, 98.

[28] F. Ahmed, D. E. Discher, *J. Controlled Release* **2004**, *96*, 37.

[29] R. Nagarajan, *Polym. Adv. Technol.* **2001**, *12*, 23.

[30] P. Alexandridis, B. Lindman, *Amphiphilic Block Copolymers: Self-Assembly and Applications*, Elsevier, Amsterdam **2000**.

[31] H. Chen, S. Kim, L. Li, S. Wang, K. Park, J. X. Cheng, *Proc. Natl. Acad. Sci. U. S. A.* **2008**, *105*, 6596.

[32] M. Xie, S. Wang, A. Singh, T. J. Cooksey, M. D. Marquez, A. Bhattarai, K. Kourentzi, M. L. Robertson, *Soft Matter* **2016**, *12*, 6196.

[33] J. Lu, S. C. Owen, M. S. Shoichet, *Macromolecules* **2011**, *44*, 6002.

[34] Rasband, W.S. ImageJ. U. S. National Institutes of Health, Bethesda, MD. https://imagej.nih.gov/ij/.

[35] C. A. Schneider, W. S. Rasband, K. W. Eliceiri, *Nat. Methods* **2012**, *9*, 671.

[36] M. D. Abramoff, P. J. Magalhaes, S. Ram, *J. Biophotonics Int.* **2004**, *11*, 36.

[37] Y. Yamamoto, K. Yasugi, A. Harada, Y. Nagasaki, K. Kataoka, *J. Controlled Release* **2002**, *82*, 359.

[38] H. Fan, Y. Li, J. Yang, X. Ye, *J. Phys. Chem. B* **2017**, *121*, 9708.

[39] C. R. Heald, S. Stolnik, K. S. Kujawinski, C. De Matteis, M. C. Garnett, L. Illum, S. S. Davis, S. C. Purkiss, R. J. Barlow, P. R. Gellert, *Langmuir* **2002**, *18*, 3669.

[40] H. Chen, S. Kim, W. He, H. Wang, P. S. Low, K. Park, J. X. Cheng, *Langmuir* **2008**, *24*, 5213.

[41] S. Jiwpanich, J.-H. Ryu, S. Bickerton, S. Thayumanavan, *J. Am. Chem. Soc.* **2010**, *132*, 10683.

[42] S. C. Owen, D. P. Y. Chan, M. S. Shoichet, *Nano Today* **2012**, *7*, 53.

[43] P. Rajdev, S. Ghosh, *J. Phys. Chem. B* **2019**, *123*, 327.

[44] Y. V. Malyukin, S. L. Efimova, K. Kemnitz, *J. Lumin.* **2001**, *94*, 239.

[45] S. L. Yefimova, G. Y. Gural'chuk, A. V. Sorokin, Y. V. Malyukin, I. A. Borovoy, A. S. Lubyanaya, *J. Appl. Spectrosc.* **2008**, *75*, 658.

SUPPORTING INFORMATION

Additional supporting information may be found online in the Supporting Information section at the end of this article.